

Parametrization of Crystal Field Splittings of the 7F_J Levels in Eu^{3+} Doped Tetragonal Rare Earth Oxyhydroxides, $\text{REOOH}:\text{Eu}^{3+}$ ($\text{RE} = \text{Y}$ and Lu)

Jorma Hölsä

Department of Chemical Engineering, Helsinki University of Technology, SF-02150 Espoo, Finland

Z. Naturforsch. **45a**, 173–178 (1990); received October 23, 1989

The luminescence spectra of europium($3+$) doped rare earth oxyhydroxides, $\text{REOOH}:\text{Eu}^{3+}$ ($\text{RE} = \text{Y}$ and Lu), were studied and analyzed at 77 and 300 K under UV and dye laser excitation. The observed ${}^7F_{0-4}$ level schemes were simulated with the aid of the phenomenological crystal field theory. The descending symmetry method from C_{2v} to C_s symmetry was used in the simulation. Good results were obtained with C_s symmetry simulation which yielded r.m.s. deviations of 6 and 7 cm^{-1} between the calculated and experimental ${}^7F_{0-4}$ level schemes for $\text{YOOH}:\text{Eu}^{3+}$ and $\text{LuOOH}:\text{Eu}^{3+}$, respectively. The C_{2v} simulation was found inadequate to describe the experimental energy level schemes. The even rank crystal field parameters vary only slightly as a function of the host. Comparison with the corresponding values obtained for the monoclinic form of the Eu^{3+} doped RE oxyhydroxides reveals significant differences.

Key words: Crystal field, Europium, Rare earth oxyhydroxides.

Introduction

Ever since the rapid development in the research of rare earth based phosphors in 1960's [1–3] the RE oxysalts have played an important role both in science and in industrial applications. RE oxysalts have found useful applications as colour TV phosphors (e.g. $(\text{YO})_2\text{S}:\text{Eu}^{3+}$ [4]) and x-ray intensifying screens (e.g. $\text{REOX}:\text{Tb}^{3+}$ [5]). The static and dynamic luminescence properties of these phosphors have intensively been studied [6–9]. Some other RE oxysalt phosphors have also received scientific attention [10–16]. Their possible use in large scale industrial applications is, however, not in foresight. Anyhow, such studies have raised the question whether the structurally very stable $(\text{REO})_n^{n+}$ complex cation has an imposing role also in determining the luminescence properties of these oxysalts [17]. The existence of rigid and strongly bonded entities has been proposed not only for the RE oxysalts [18] but also for RE hydroxo and sulfide compounds [19].

This study is a continuation to our investigations conducted on RE oxysalts [9, 10, 13–15] and a complement to the preliminary report on the differences in luminescence properties between the Eu^{3+} doped monoclinic and tetragonal RE oxyhydroxides [20].

Reprint requests to Prof. Dr. Ing. Jorma Hölsä, Department of Chemical Engineering, Helsinki University of Technology, SF-02150 Espoo, Finland.

Crystal Structure of Tetragonal RE Oxyhydroxides

The high pressure and temperature modification of RE oxyhydroxides have tetragonal structure with $P4_21m\text{-}D_{2d}^3$ (no. 113 in [21]) as the space group [22]. The unit cell (with $a=5.465$ and $c=5.327\text{ Å}$ for YbOOH [22]) contains four molecular units. A complete crystal structure determination is available only for the ytterbium compound but the whole REOOH series (except LaOOH , which has not yet been synthesized) has been shown to be isomorphic [23]. Accordingly, the following considerations are valid for YOOH and LuOOH , too, while remembering the general trend of increasing distortions of the idealized structure with increasing ionic radius of the RE^{3+} ion [24].

RE atoms occupy in tetragonal REOOH a single site with C_s symmetry. The RE atoms are seven coordinated to four oxygens and to the three oxygens from hydroxyl groups. The seven oxygens form a distorted monocapped trigonal prism as the coordination polyhedron around the RE atom. The Yb-O distances vary from 2.219 to 2.446 Å which indicates important distortions from the C_{2v} , being the next higher symmetry from C_s . These distortions exceed 0.23 Å in Yb-O distances, which is clearly more than in the monoclinic low pressure and temperature form of HoOOH [25].

0932-0784 / 90 / 0200-0173 \$ 01.30/0. – Please order a reprint rather than making your own copy.



Dieses Werk wurde im Jahr 2013 vom Verlag Zeitschrift für Naturforschung in Zusammenarbeit mit der Max-Planck-Gesellschaft zur Förderung der Wissenschaften e.V. digitalisiert und unter folgender Lizenz veröffentlicht: Creative Commons Namensnennung-Keine Bearbeitung 3.0 Deutschland Lizenz.

Zum 01.01.2015 ist eine Anpassung der Lizenzbedingungen (Entfall der Creative Commons Lizenzbedingung „Keine Bearbeitung“) beabsichtigt, um eine Nachnutzung auch im Rahmen zukünftiger wissenschaftlicher Nutzungsformen zu ermöglichen.

This work has been digitalized and published in 2013 by Verlag Zeitschrift für Naturforschung in cooperation with the Max Planck Society for the Advancement of Science under a Creative Commons Attribution-NoDerivs 3.0 Germany License.

On 01.01.2015 it is planned to change the License Conditions (the removal of the Creative Commons License condition "no derivative works"). This is to allow reuse in the area of future scientific usage.

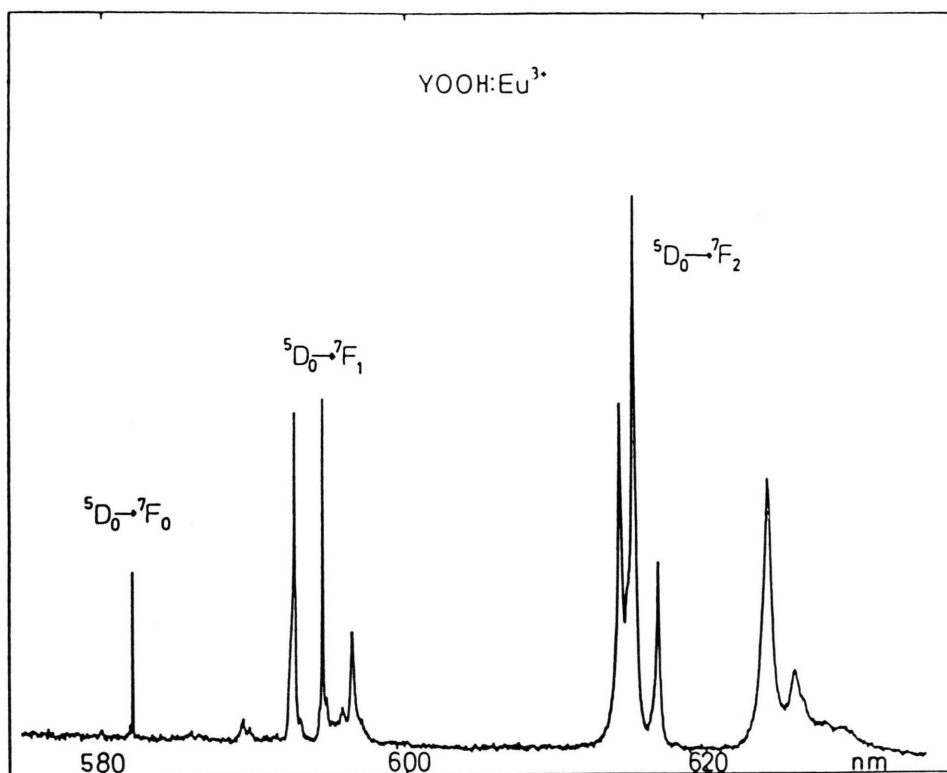


Fig. 1. Part of the emission spectrum of tetragonal YOOH:Eu³⁺ at 77 K under UV excitation.

Experimental Section

The tetragonal modification of yttrium and lutetium oxyhydroxides were obtained in polycrystalline powder form by applying a pressure of 4 to 6 GPa and a temperature of 1050 K on moist Y₂O₃ and Lu₂O₃ of 4 N purity. The "belt" type apparatus used was similar to that employed in [22]. The purity of the products was controlled with routine x-ray powder diffraction which showed no presence of other phases. The RE oxides used in synthesis as starting materials were doped with a small amount – nominally 1 mole per cent – of Eu³⁺ ion. The distribution of the Eu³⁺ ions replacing the host cation was assumed to remain random and uniform after the pressure and temperature treatment, too.

The luminescence of REOOH:Eu³⁺ powder samples was obtained either under a conventional UV lamp or a rhodamine dye laser excitation. A 200 W mercury lamp equipped with wide band filters provided UV radiation between 250 and 300 nm. This wavelength region excites to the strongly absorbing charge transfer absorption band of the Eu³⁺ ion in REOOH.

A Spectra Physics 164 argon ion laser pumped a Spectra Physics 375/376 continuous wave dye laser (with rhodamine 6G as the dye) providing intense orange light used to excite selectively the lowest excited ⁵D level, ⁵D₀, near 580 nm. In order to profit from the narrowing of the transition lines at low temperatures, the luminescence was studied both at ambient and liquid nitrogen temperatures. The liquid nitrogen temperature was achieved by immersing the REOOH:Eu³⁺ powder samples in liquid nitrogen in a quartz sample holder. The emission was dispersed by a 1-m Jarrell-Ash monochromator and detected by a Hamamatsu R 374 photomultiplier. The luminescence spectra were recorded in the wavelength region between 400 and 750 nm.

Analysis of the Luminescence Spectra

Part of the UV excited luminescence spectrum of YOOH:Eu³⁺ is displayed in Figure 1. The energies of the peaks in the whole spectrum between 580 and 720 nm are reported in Table 1. The luminescence of REOOH:Eu³⁺ arises practically alone from transi-

Table 1. Energies of the $^5D_0 \rightarrow ^7F_{0-4}$ transitions observed in the emission spectrum of tetragonal REOOH:Eu $^{3+}$ (RE=Y and Lu) (in cm $^{-1}$ units).

Transition	YOOH:Eu $^{3+}$	LuOOH:Eu $^{3+}$
$^5D_0 \rightarrow ^7F_0$	17 178	17 166
$^5D_0 \rightarrow ^7F_1$	16 871	16 850
	16 818	16 820
	16 762	16 750
$^5D_0 \rightarrow ^7F_2$	16 276	16 264
	16 251	16 251
	16 209	16 206
	16 017	15 999
	15 972	15 961
$^5D_0 \rightarrow ^7F_3$	15 328	15 315
		15 283
	15 284	15 279
	15 268	15 264
	15 234	15 217
	15 202	15 193
	15 160	15 142
$^5D_0 \rightarrow ^7F_4$	14 531	14 531
	14 454	14 453
		14 347
	14 280	14 265
	14 263	14 250
	14 221	14 204
	14 147	14 127
	14 137	14 112
	14 119	14 101

tions from the 5D_0 level to the ground multiplet, 7F_J , $J=0-4$. In spite of the low concentration of the Eu $^{3+}$ ions – rendering the concentration quenching inefficient – transitions from the higher 5D_J ($J=1-4$) are quenched to 5D_0 level. The main path of relaxation of the excitation energy seems to be the multiphonon de-excitation. The few high frequency phonons needed to cover the energy gap of a few 1000 cm $^{-1}$ between the different 5D levels are readily furnished by the OH lattice vibrations.

The crystal field effect produces no splitting of the 5D_0 and 7F_0 levels, and thus in the presence of a single luminescent phase only a single $^5D_0 \rightarrow ^7F_0$ transition should be observed. In fact this is the case of the luminescence spectrum of YOOH:Eu $^{3+}$ (cf. Fig. 1) where a sharp, isolated peak at 582.1 nm was found. The high intensity of this transition is consistent with the low point symmetry of the Eu $^{3+}$ site (C_s) as given by the structural data. The electronic transition selection rules for both magnetic and electric dipole induced transition allow no transition between levels with $J=0$. The introduction of a RE $^{3+}$ ion into a crystalline environment, however, breaks down the electronic transition selection rules, and the group

theoretical selection rules left valid allow the $^5D_0 \rightarrow ^7F_0$ transition for the site symmetries C_s , C_n and C_{nv} [26].

In addition to the $^5D_0 \rightarrow ^7F_0$ transition the $^5D_0 \rightarrow ^7F_{1-4}$ transitions can be observed as well. The magnetic dipole induced $^5D_0 \rightarrow ^7F_1$ transition (selection rule $\Delta J=0, \pm 1$) has an equal strength with the hyper-sensitive, mostly electric dipole induced $^5D_0 \rightarrow ^7F_2$ transition. The electric dipole induced transitions follow the selection rule $\Delta J=\pm 2, \pm 4$ and ± 6 for the initial state with $J=0$. The presence of the intense $^5D_0 \rightarrow ^7F_4$ transition is consistent with this selection rule while the forbidden $^5D_0 \rightarrow ^7F_3$ transition gains strength only by the mixing of the 7F_J wave functions by the crystal field effect [27]. This transition thus possesses a mixed magnetic/electric dipole character. The number of the lines for each $^5D_0 \rightarrow ^7F_J$ ($J=0, 1, 2, 3$ and 4) transition – 1, 3, 5, 7 and 9 (for LuOOH:Eu $^{3+}$), respectively – reveals the total lifting of the $(2J+1)$ degeneracy of the 7F_J levels. This observation is consistent with the C_s site symmetry which generates no selection rules between the different Stark sublevels, either [28]. The emission spectra of the Eu $^{3+}$ ion are closely similar in both REOOH matrices, as should be evident on the grounds of the structural isomorphism. A shift in the excited levels to higher energy – called the nephelauxetic effect – is, however, clearly visible as a function of the RE host cation (Table 1).

Although the different modifications of the RE oxyhydroxides are not strictly isomorphic the RE coordination are closely related. Thus it is interesting to compare the 7F_J energy level schemes of the Eu $^{3+}$ ion in the two forms of the same RE oxyhydroxide. The energy level schemes of YOOH:Eu $^{3+}$ reproduced in Fig. 2, reveal the general resemblance of the two schemes. The total crystal field splittings of the tetragonal form are, however, significantly compressed in comparison to those of the monoclinic form. This indicates the compressing effect of the external pressure applied during the preparation on the energy level scheme of the Eu $^{3+}$ ion. In contrast to the total splittings of the 7F_J levels the splittings between the individual Stark components are markedly smaller in the monoclinic form. This observation reflects the effect of the increased distortions of the RE coordination in the tetragonal form. Accordingly, it should be concluded that a successful treatment of the $^7F_{0-4}$ energy level schemes in terms of a symmetry higher than C_s seems rather improbable.

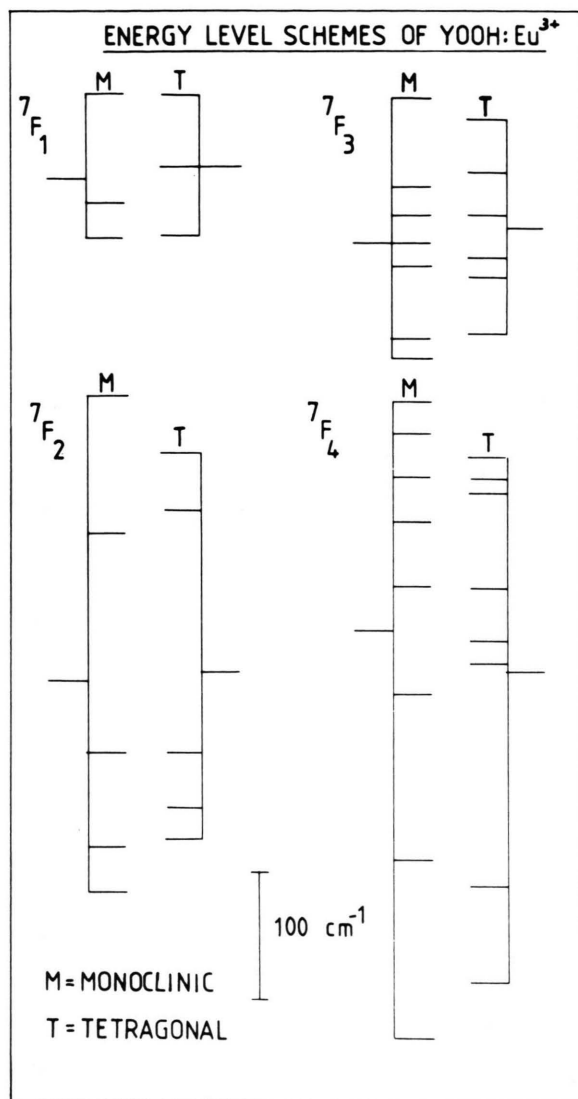


Fig. 2. Comparison between the experimental crystal field splittings of ${}^7F_{0-4}$ levels of monoclinic and tetragonal YOOH:Eu $^{3+}$.

Crystal Field Simulation of the ${}^7F_{0-4}$ Level Schemes

The $4f^6$ configuration of the Eu $^{3+}$ ion has a total of 3003 $|SLMJ\rangle$ Stark sublevels. Since the treatment of the $4f^6$ configuration as a whole seems impractical the usual way is to introduce some kind of a truncation of the wave functions. The simplest way is to take into account only the 49 components of the ${}^7F_{0-6}$ ground multiplet. Such a rather drastic truncation naturally neglects many minor perturbations on the 7F_J wave functions. The restricted set of 7F_J wave functions has

Table 2. Experimental and calculated ${}^7F_{0-4}$ energy level schemes of tetragonal REOOH:Eu $^{3+}$ (in cm^{-1} units).

Level	YOOH:Eu $^{3+}$			LuOOH:Eu $^{3+}$		
	Exp.	Calc. C_{2v}	C_s	Exp.	Calc. C_{2v}	C_s
7F_0 A_1	0	0	0	0	0	0
7F_1	B_2	307	316	316	318	317
	B_1	360	358	346	354	348
	A_2	416	411	416	406	413
7F_2	A_1	902	894	902	889	892
	B_2	927	925	915	919	924
	A_2	969	963	971	960	958
	A_1	1161	1178	1167	1178	1171
	B_1	1206	1205	1205	1209	1205
7F_3	B_2	1850	1854	1850	1851	1846
	B_1		1875	1882	1883	1885
	A_2	1894	1902	1899	1887	1895
	A_1	1910	1909	1910	1902	1913
	B_2	1944	1945	1947	1949	1947
	A_2	1978	1968	1971	1973	1965
	B_1	2018	2016	2017	2024	2023
7F_4	A_1	2647	2657	2647	2635	2651
	A_2	2724	2720	2726	2713	2714
	B_1		2795	2870	2819	2812
	B_2	2898	2891	2895	2901	2898
	B_1	2915	2921	2913	2916	2923
	A_1	2957	2960	2958	2962	2966
	B_2	3031	3022	3031	3054	3050
	A_1	3041	3038	3041	3039	3024
	A_2	3059	3062	3059	3065	3065
						3067

in most cases been found sufficient to describe in an adequate way the effect of the neighboring atoms on the electronic structure of the Eu $^{3+}$ ion. The success encountered originates from two facts: firstly, the 7F_J ground multiplet is energetically well separated (nearly $12\,000\text{ cm}^{-1}$) from the next highest excited multiplet (${}^5D_{0-4}$) and secondly the crystal field operator mixes only wave functions with the same multiplicity (the 7F septet is the only one within the $4f^6$ configuration). In view of the reasoning presented above the phenomenological crystal field simulation of the ${}^7F_{0-4}$ level schemes in REOOH:Eu $^{3+}$ was carried out on the basis set of 49 ${}^7F_{JM}$ wave functions.

According to Wybourne's formalism [2] the crystal field Hamiltonian can be expressed as a sum of the products between the real and imaginary crystal field parameters (B_q^k and S_q^k) and the spherical harmonics (C_q^k):

$$H_{\text{cf}} = \sum_{k,q} [B_q^k (C_q^k + C_{-q}^k) + i S_q^k (C_q^k - C_{-q}^k)].$$

The even part of the crystal field Hamiltonian for the C_s symmetry includes the following nine real B_q^k parameters which are also the parameters corre-

Table 3. The values of the even rank crystal field B_k^q parameters (all values in cm^{-1} units) for tetragonal REOOH:Eu³⁺. The numbers in parentheses refer to the standard deviation of the parameters.

Parameter	YOOH:Eu ³⁺		LuOOH:Eu ³⁺	
	C _{2v}	C _s	C _{2v}	C _s
B_0^2	234 (27)	258 (26)	212 (28)	242 (45)
B_2^2	50 (16)	55 (20)	46 (17)	30 (19)
B_0^4	121 (44)	122 (44)	165 (44)	148 (53)
B_2^4	1399 (21)	1382 (29)	1407 (22)	1351 (33)
S_2^4		-64 (22)		204 (27)
B_4^4	9 (30)	94 (31)	-48 (31)	-44 (33)
S_4^4		63 (32)		176 (38)
B_0^6	-381 (47)	-386 (60)	-477 (50)	-517 (69)
B_2^6	141 (31)	132 (46)	192 (29)	236 (41)
S_2^6		352 (46)		396 (46)
B_4^6	265 (33)	268 (40)	223 (32)	160 (40)
S_4^6		74 (30)		83 (36)
B_6^6	-49 (29)	-21 (28)	-31 (30)	36 (36)
S_6^6		198 (33)		110 (34)
S		406		407
r.m.s. deviation	8.6	6.0	9.7	6.5

The crystal field calculations were carried out with the matrix diagonalization and least squares refinement programs REEL (only real crystal field parameters) and IMAGE (including the imaginary parameters as well) [30]. The crystal field strength parameter S was calculated according to [31].

sponding to the supergroup (C_{2v}) of the C_s symmetry [28]:

$$B_0^2, B_0^4, B_0^6, B_2^2, B_2^4, B_2^6, B_4^4, B_4^6, \text{ and } B_6^6.$$

The total number of even parameters for the C_s symmetry is 14 of which five are imaginary ones, namely

$$S_2^4, S_2^6, S_4^4, S_4^6, \text{ and } S_6^6.$$

Since the amount of the experimental data consists of only the 25 $^7F_{0-4}$ level energies, the crystal field simulation was carried out according to the descending symmetry method [29]. The symmetry considered first was C_{2v} with only nine real B_k^q parameters. The results of this simulation proved to be unsatisfactory as the r.m.s. deviations around 10 cm^{-1} indicate (Table 3). The situation is in contrast to that of the monoclinic REOOH:Eu³⁺ where the C_{2v} symmetry simulation yielded much better results except with LaOOH:Eu³⁺ [32]. The better C_{2v} symmetry simulation with the monoclinic form reflects the more regular RE coordination close to the C_{2v} symmetry, as discussed above.

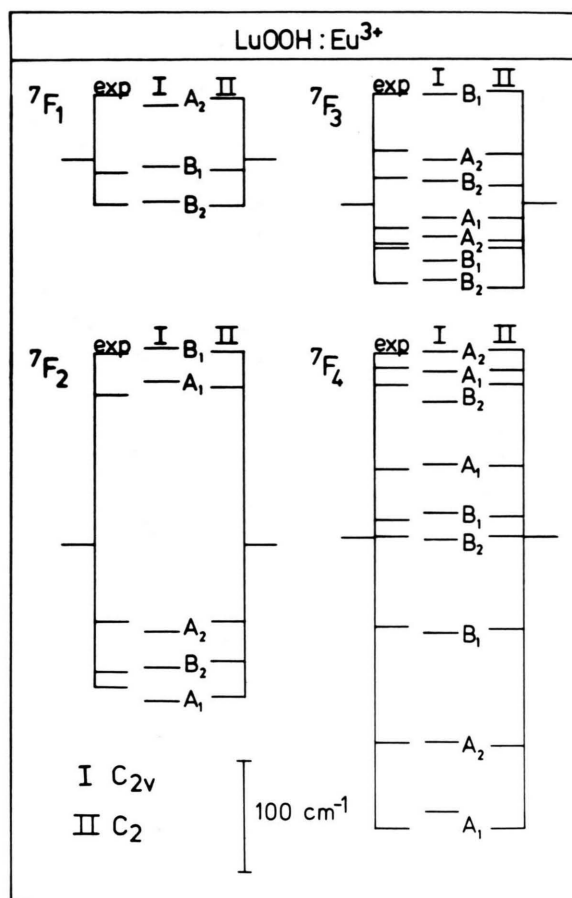


Fig. 3. Comparison between the calculated and experimental crystal field splittings of $^7F_{0-4}$ levels of LuOOH:Eu³⁺.

The introduction of five additional imaginary parameters inherent in the C_s symmetry reduced considerably the r.m.s. deviations in both matrices studied (Table 3). The magnitude of the imaginary parameters differs significantly from zero, too, and thus the better simulation can be concluded to result from taking into account the requirements imposed by the low symmetry. The purely statistic effect of the increasing number of parameters can thus be ruled out. The better fit between the experimental and calculated energy level schemes can be seen in Fig. 3, too.

The best fit parameter sets are characterized by small second rank parameter values as was concluded from the weak splitting of the 7F_1 level. This can be taken as an indication of the weakness of the electrostatic field created by the oxygens in the immediate environment of the Eu³⁺ ion [33]. The fourth and

sixth rank parameters assumed important values. From these results it may be concluded that the short range crystal field effects dominate in REOOH:Eu³⁺ material. One could argue also that the "covalent" bonding plays an important role in these compounds.

A comparison with the parameter sets obtained for the monoclinic form of REOOH reveals significant differences mainly in the B_0^4 values. The differences could be anticipated because of the distorted coordination of the RE cation in tetragonal REOOH. The effect of distortions seen in Fig. 2 was discussed more closely above. In spite of the good simulation of the ${}^7F_{0-4}$ energy level schemes some of the spectral characteristics are left unresolved. The most important problem is the high intensity of the ${}^5D_0 \rightarrow {}^7F_0$ transition. In a few occasions [13, 27] it has been shown that this transition gains strength through the mixing of mainly the ${}^7F_{2M}$ components in the ${}^7F_{00}$ wave function. As a consequence of the small second rank parameter values the amount of the other ${}^7F_{JM}$ components in the ${}^7F_{00}$ wave function do not exceed a few per cent. This low contribution can not be considered as sufficient to explain the intense ${}^5D_0 \rightarrow {}^7F_0$ transition. At the moment this problem seems to remain unresolved until more elaborate theories are presented.

The comparison of the results of the crystal field analysis of REOOH:Eu³⁺ with the results ob-

tained for REOCl:Eu³⁺ [13], REOBr:Eu³⁺ [34], (REO)₂SO₄:Eu³⁺ [14] and (REO)₂MO₄:Eu³⁺ (M = Mo and W) [16] shows fundamental differences. The compounds above form a uniform group with similar spectroscopical properties characterized by strong second rank parameter values. This is in drastic contrast to REOOH:Eu³⁺ and it must be concluded that the strong bonded (REO)_n⁺ entity can not exist in REOOH. Quite recently an interesting proposal has been presented concerning the existence of common structural units also in RE hydroxosalts and sulphides [19]. The dominant unit in REOOH may thus be the RE(OH)²⁺ group rather than the (REO)_n⁺ one. The verification of the hypothesis that RE oxyhydroxides can be considered as prototypes of RE hydroxosalts has to be left to later studies of the other members of this group, e.g. RE(OH)₂X, X = Cl and Br.

Acknowledgements

The author is indebted to Dr. C. Chateau (U.P.R. 211, C.N.R.S., Meudon France) for the preparation of the rare earth oxyhydroxide samples. The author wishes to present further thanks to Dr. P. Caro and Dr. P. Porcher (U.P.R. 210, C.N.R.S., Meudon France) for the use of the spectroscopic equipment and the matrix diagonalization program for crystal field calculations. Financial aid from the Academy of Finland is gratefully acknowledged.

- [1] G. H. Dieke, Spectra and energy levels of rare earth ions in crystals, Interscience, New York 1968.
- [2] B. G. Wybourne, Spectroscopic Properties of Ions in Crystals, Interscience, New York 1965.
- [3] R. D. Peacock, Struct. Bond. **22**, 83 (1975).
- [4] A. E. Hardy, IEEE Trans. El. Dev. **ED-15**, 868 (1968).
- [5] J. G. Rabatin, Proc. 12th Rare Earth Res. Conf., Vail 1976, p. 819.
- [6] O. J. Sovers and T. Yoshioka, J. Chem. Phys. **51**, 5330 (1969).
- [7] O. J. Sovers, M. Ogawa, and T. Yoshioka, J. Lumin. **18/19**, 336 (1979).
- [8] J. Dexpert-Ghys, Y. Charreire, M. Leskelä, and L. Niinistö, J. Electrochem. Soc. **132**, 711 (1985).
- [9] J. Hölsä and P. Porcher, J. Chem. Phys. **76**, 2798 (1982).
- [10] J. Hölsä and P. Porcher, J. Less-Common Met. **112**, 127 (1985).
- [11] O.-K. Moune-Minn and P. Caro, J. Crystallogr. Spectrosc. Res. **12**, 157 (1982).
- [12] O.-K. Moune-Minn, P. Porcher, and P. Caro, J. Solid State Chem. **50**, 41 (1983).
- [13] J. Hölsä and P. Porcher, J. Chem. Phys. **75**, 2108 (1981).
- [14] P. Porcher, D. R. Svoronos, M. Leskelä, and J. Hölsä, J. Solid State Chem. **46**, 101 (1983).
- [15] J. Hölsä, T. Leskelä, and M. Leskelä, Inorg. Chem. **24**, 1539 (1985).
- [16] J. Huang, J. Lories, and P. Porcher, J. Solid State Chem. **43**, 87 (1982).
- [17] P. Porcher and P. Caro, J. Less-Common Met. **93**, 151 (1983).
- [18] P. Caro, C. R. Acad. Sci. Paris **C 262**, 992 (1966).
- [19] G. M. Kuzmicheva, I. V. Perelkin, and A. A. Eliseev, Russ. J. Inorg. Chem. **29**, 2690 (1984).
- [20] J. Hölsä, C. Chateau, T. Leskelä, and M. Leskelä, Acta Chem. Scand. **A 39**, 415 (1985).
- [21] International Tables for X-ray Crystallography, Vol. I, Kynoch Press, Birmingham 1974.
- [22] A. Norlund Christensen and R. G. Hazell, Acta Chem. Scand. **26**, 1171 (1972).
- [23] M. Gondrand and A. Norlund Christensen, Mater. Res. Bull. **6**, 239 (1971).
- [24] G. A. Bandurkin, B. F. Bzhurinskii, Inorg. Mater. **9**, 64 (1973).
- [25] A. Norlund Christensen, Acta Chem. Scand. **19**, 1391 (1965).
- [26] B. R. Judd, J. Chem. Phys. **44**, 839 (1966).
- [27] P. Porcher and P. Caro, J. Lumin. **21**, 207 (1980).
- [28] J. L. Prather, N.B.S. Monograph **19** (1961).
- [29] J. Hölsä and M. Leskelä, Mol. Phys. **54**, 657 (1985).
- [30] P. Porcher, unpublished work.
- [31] N. C. Chang, J. B. Gruber, R. P. Leavitt, and C. A. Morrison, J. Chem. Phys. **76**, 3877 (1982).
- [32] J. Hölsä, (in press). J. Phys. Chem.
- [33] J. Dexpert-Ghys, M. Faucher, and P. Caro, Phys. Rev. **B 23**, 607 (1981).
- [34] J. Hölsä and P. Porcher, J. Chem. Phys. **76**, 2790 (1982).